Applied Energy 183 (2016) 160–169

Contents lists available at ScienceDirect

Applied Energy

journal homepage: www.elsevier.com/locate/apenergy

Determining the size of PHEV charging stations powered by commercial grid-integrated PV systems considering reactive power support

Duong Quoc Hung [a,*], Zhao Yang Dong [b], Hieu Trinh [a]

[a] School of Engineering, Deakin University, VIC 3216, Australia
[b] School of Electrical and Information Engineering, The University of Sydney, NSW 2006, Australia

HIGHLIGHTS

- Penetration of commercial grid-connected PV and PHEVs for minimizing energy losses.
- Sizing of PV powered workplace charging stations and their reactive power support.
- Consideration of the probabilistic characteristic of PV generation.
- Impacts of time-varying voltage-dependent charging load models on PV penetration.
- Analyses of probabilistic voltage distributions and peak load demand reduction.

ARTICLE INFO

Article history:
Received 2 July 2016
Received in revised form 18 August 2016
Accepted 28 August 2016

Keywords:
Distributed generation
Energy loss
Plug-in hybrid electric vehicle
Probabilistic reactive power
Solar photovoltaic
Time-varying commercial charging load model

ABSTRACT

Due to low electricity rates at nighttime, home charging for electric vehicles (EVs) is conventionally favored. However, the recent tendency in support of daytime workplace charging that absorbs energy produced by solar photovoltaic (PV) panels appears to be the most promising solution to facilitating higher PV and EV penetration in the power grid. This paper studies optimal sizing of workplace charging stations considering probabilistic reactive power support for plug-in hybrid electric vehicles (PHEVs), which are powered by PV units in medium voltage (MV) commercial networks. In this study, analytical expressions are first presented to estimate the size of charging stations integrated with PV units with an objective of minimizing energy losses. These stations are capable of providing reactive power support to the main grid in addition to charging PHEVs while considering the probability of PV generation. The study is further extended to investigate the impact of time-varying voltage-dependent charging load models on PV penetration. The simulation results obtained on an 18-bus test distribution system show that various charging load models can produce dissimilar levels of PHEV and PV penetration. Particularly, the maximum energy loss and peak load reductions are achieved at 70.17% and 42.95% respectively for the mixed charging load model, where the system accommodates respective PHEV and PV penetration levels of 9.51% and 50%. The results of probabilistic voltage distributions are also thoroughly reported in the paper.

1. Introduction

Solar photovoltaic (PV) has received remarkable worldwide attention over the past decade [1]. The global installed capacity was approximately 178 GW at the end of 2014 and this amount is expected to be more than 540 GW by 2019. Meanwhile, the usage of electric vehicles (EVs) has been growing in many parts of the world such as the United States, Japan, China and Europe due to their environmental benefits, advancements in the technology, battery cost reductions, and government incentives [2]. It has been reported that the total worldwide EVs stock was over 0.02% (0.18 million units) of the total passenger cars through 2012. This figure is projected to increase to 2% (20 million) by 2020. Furthermore, an online survey has been recently conducted in the United States to evaluate the possibility of the economic and environmental benefits obtained from EV and renewable energy deployment [3]. This investigation indicated that there would be an increase of 433% in the usage of public charging stations if renewable energy resources, including solar PV generation were offered.

The widespread adoption of intermittent solar PV sources can increase the pressure on the distribution system, especially power fluctuations, reverse power flows, voltage rises and high power losses [4]. In contrast, the distribution system would potentially face excessive voltage drops, feeder overloads and high network

* Corresponding author.
E-mail address: hung.duong@deakin.edu.au (D.Q. Hung).

http://dx.doi.org/10.1016/j.apenergy.2016.08.168
0306-2619/

losses caused by high EV penetration [5]. However, EV charging loads can support high PV penetration while mitigating dependence and impacts on the power grid, the intermittency of PV production and emissions as well [6,7]. This coordination is also expected to meet the demand for daytime charging at workplace parking infrastructures [8–10].

The study of EV charging stations consuming energy produced by grid-connected PV panels at workplace parking areas during the daytime has been conducted in a number of recent research efforts [11–27]. This model has comprehensively reported to bring multiple technical and economic benefits to vehicle and garage owners and power utilities. In [11], the benefits of EV charging facilities powered by PV panels were quantified using an optimal charging algorithm, which was developed based on dynamic programming and rule-based control. This analysis showed that daytime charging based on solar PV at workplace generated a lower charging cost than nighttime home charging without solar energy while the garage owner gained a reasonable profit. Other possible benefits included lower emissions and power consumption from the grid and higher PV penetration. Moreover, a research [12] emphasized that coordinated operation of both PV and PHEVs during the mid-day can enable higher penetration levels of not only PV, but also EVs during low demand periods and less curtailment of surplus PV production. Meanwhile, a study [13] designed a charging facility supplied by PV panels to maximize the consumption of PV power while minimizing voltage deviations in distribution networks. In this work, a real-time fuzzy logic controller that incorporates a probabilistic model was proposed to forecast PV generation and PHEV charging loads. Such a method was also employed to control multiple charging stations to minimize charging costs, network power losses and voltage deviations in MV industrial/commercial power networks [14]. In [15], an optimal EV charging approach based on forecasted PV generation load demand was also presented to reduce the electricity cost in commercial buildings. Similarly, a mixed-integer linear programming approach was presented to minimize the annual energy cost and emission while enabling high PV penetration in commercial buildings involving EVs [16]. An concept of a future smart city was also developed in [17], where EVs are charged using power generated from PV panels to reduce electricity demand. Recently, a study [18] reported a heuristic operation approach that accommodate EVs and PV panels to enhance the self-consumption of PV power in commercial buildings and a research [19] showed optimal EV charging using PV panels to reduce dependency on the grid and maximize the usage of solar energy as well. A coordinated charging approach was proposed to enable operational synergy between PV generation and EV charging and subsequently reduce emissions in an urban distribution network [20]. An online energy management for PV-assisted charging stations was developed to maximize the self-consumption of PV and decide the power supplied from the grid under time-of-use pricing [21]. A smart charging model was presented to increase the self-consumption of PV power using EV charging loads and reduce peak load demand [22]. In [23], a PV-powered charging station was proposed to reduce the intermittency of PV production and the cost of energy trading to the charging station. In [24], economic operation of a microgrid-like EV parking deck powered by PV panels was also presented to minimize the intermittency of PV generation while maximizing the total revenue. In addition, an experiment on a microgrid-connected charging station, which involves solar and wind sources and energy storage buffers, demonstrated a reduction in energy exchange between EV charging and the main grid [25]. Another experimental study showed that PV-powered charging stations significantly declined the energy consumption from the grid [26]. More importantly, an uncoordinated charging approach was successfully developed using a stochastic model that considers load demand, EV charging and PV generation in an urban power network [27]. This study observed that daytime charging combined with PV generation can enhance load and voltage profiles despite the fact that no optimal charging algorithms and control devices were employed.

The aforementioned survey shows that sufficient work has been done with respect to the optimal control of EV charging stations powered by grid-connected PV systems; two key shortcomings unresolved, however, were identified. Firstly, the existing studies have assumed that the sizes of PV units and charging stations are pre-specified. Such an assumption may lead to a possibility of an under/over-estimation of the penetration of PV and EVs. Consequently, the power network may experience excessive increases in reverse power flows, power losses and voltage variations. Secondly, the ability to provide probabilistic reactive power support by PV units and EVs was also neglected in the above-reviewed studies. The immediate concern is that given high intermittent PV penetration with active power provision only together with sharply increased charging loads, the deficiency of reactive power support may exist in the distribution network. Switchable capacitor banks are conventionally employed for reactive power compensation. Nevertheless, they are not adequately fast to compensate for transient events as a consequence of the intermittency of PV generation and the voltage rise that occurs due to reverse power flow when the generation of PV exceeds the local demand [28,29]. As fast response devices, inverter-based charging stations powered by PV panels are permitted to regulate reactive power to stabilize load voltages while charging EVs as a primary task [30,31]. Overall, depending on the nature of loads, if properly sized, PV powered charging stations that are capable of reactive power provision may have positive effects on reducing energy losses and stabilizing bus voltages as well.

The contribution of this paper is to propose a new analytical approach to determine the size of PHEV charging stations powered by different levels of grid-connected PV penetration that considers probabilistic reactive power support for energy loss reduction. To this end, expressions are first developed to estimate the size of PV powered charging stations that can provide reactive power support for minimizing energy losses while considering the probability of PV generation. The proposed expressions are achieved by significantly expanding the previous work [32], where an analytical expression was derived from an exact loss formula for DG allocation only at the peak load to reduce power losses without consideration of EVs and their probabilistic reactive power support. The proposed approach is further extended to study the effect of charging loads on PV penetration. Various charging levels (i.e., normal, fast and mixed) are defined by time-varying voltage-dependent commercial charging load models. Moreover, the paper shows the importance of charging loads and the reactive power response of charging stations in reducing energy losses, peak loads and voltage deviations. Some interesting findings of PHEV and PV penetration levels with various commercial charging load models are reported as well.

The rest of this paper is organized as follows: Section 2 describes commercial load, PHEV and PV modeling. Section 3 presents the impact of PHEVs and PV on network power and energy losses. An analytical approach to model charging stations with PV units is explained in Section 4. Section 5 shows numerical results along with discussions, followed by the conclusions and contributions of the work in Section 6.

2. Commercial load, PHEV and PV modeling

This study considers a MV power distribution network that delivers electricity to commercial customers. Their buildings are

equipped with solar PV units that are connected to the grid. PHEV charging stations are situated at the workplace parking areas and powered by the PV units. The main system components are modeled as below.

2.1. Time-varying commercial load model

The load demand of the system is assumed to follow a demand curve, which is an aggregation of various normalized daily patterns of load components: heating, cooling and ventilation, etc., as depicted in Fig. 1, where the hourly average energy demand for each load component is calculated using one-year data [33]. The peak load observed at hour 13 is 1 p.u., which is estimated as a sum of all the load components at that hour. The share of each individual component at each hour can be found in Fig. 1.

This paper considers that each bus in the studied system consists of the various components of the commercial loads mentioned before. Each of them is assumed to have individual active and reactive voltage exponents (i.e., n_p and n_q, respectively) that can be found in Table 1 and follows a respective time-varying load pattern depicted in Fig. 1. Accordingly, the voltage-dependent load model [34] that incorporates an aggregated commercial load model, which is a combination of different components of the above loads at each bus, can be defined as a time-varying voltage-dependent commercial load model. In this model, the dependence of the loads at each bus, say bus i on the voltage and time period t can be expressed as follows:

$$P_i(t) = \sum_{k=1}^{N_c} P_{oi}^k(t) \times V_i^{n_{pk}}(t) \tag{1}$$

$$Q_i(t) = \sum_{k=1}^{N_c} Q_{oi}^k(t) \times V_i^{n_{qk}}(t) \tag{2}$$

where P_{oi} and Q_{oi} correspond to the active and reactive power at bus i at nominal voltage, respectively; V_i is the voltage at bus i; k is an index (k = 1, 2, 3, … Nc), where Nc is the total number of load components that comprises commercial loads and charging loads as described below.

2.2. Commercial charging load model

The charging stations are used to charge different types of PHEVs: compact sedan, full-size sedan, mid-size SUVs and full-size SUVs. The parameters of each type, including percentage, capacity and consumption can be found in [38].

2.2.1. Hourly energy consumption

To predict hourly energy consumed by aggregated PHEVs that will arrive at a workplace and return home, a day is divided into 24-h periods. The uncertainty of arrival time is described using a normal distribution, where the mean and standard deviation are 9 and 1.5, respectively [13]. The hourly energy needed by PHEVs is estimated based on their travel distances. The uncertainty of such travel distances is described using a lognormal distribution function, where the mean and standard deviation are 3.37 and 0.5, respectively. The state of charge (SOC) is considered as the energy in percent remaining in the battery of a PHEV upon arrival. The lower and upper bounds of the SOC are 10% and 80%, respectively. As a type of plug-in hybrid electric vehicles, PHEVs are capable of working on electricity and gas using battery and internal combustion engines, respectively. In order to avoid over-discharge, the vehicles consume gas when the SOC is lower than 10%. The SOC depends on the mileage and maximum range of PHEVs. Given a mileage of a PHEV, the SOC at the beginning of a recharging cycle can be expressed as follows:

$$SOC = \begin{cases} 100 \times \left(1 - \frac{d}{d_r}\right), & d \leq d_r \\ 0, & d > d_r \end{cases} \tag{3}$$

where d corresponds to the total distance driven by a PHEV (mile); d_r is the all-electric range. The energy required to fully charge the PHEV battery can be described as follows:

$$E_b = \frac{(1 - SOC) \times BC}{\eta} \tag{4}$$

Here BC corresponds to 70% of the battery capacity (kW h) for each type of PHEVs, which is estimated as a difference between the lower and upper bounds of the SOC that were previously set at 10% and 80%, respectively; η represents the efficiency of the charger (%), which is considered to be 90%.

This study investigates two charging levels shown in Table 2, which are identified based on voltage and power levels, according to the SAE J1772 standard. In addition, it considers a mixed charging level that is defined as a mix of the normal and fast charging levels applied for sedan and SUV vehicles, respectively. Given a charging level in kW found in Table 2, the charging duration time can be estimated as the total energy consumed by PHEVs in kW h as defined by Eq. (4) divided by the charging level. To generate an hourly PHEV energy consumption for each charging level given in Table 2, a 24-h period charging load profile is made on the basis of the arrival time, energy consumption and charging level of PHEVs adopted. The total energy at any specific time is estimated as a sum of the energy required by PHEVs at that time.

2.2.2. Time-varying commercial charging load model

The time-varying voltage-dependent commercial load model expressed by Eqs. (1) and (2) that incorporates PHEV charging loads can be defined as a time-varying voltage-dependent commercial charging load model" or "time-varying commercial charging load model". In this model, n_p = 2.59 and n_q = 4.06 are the active and reactive power exponents for battery charge, respectively [35,36].

2.2.3. Charging station

The inverter-based charging station is assumed to charge PHEVs while controlling reactive power [31] under the recommendation of the latest standard IEEE 1547 [40]. In other words, the inverter-based charging station can be controlled in three quadrants. It is capable of injecting or absorbing reactive power in addition to charging PHEVs as loads. The reactive power provision from the charging station is limited as follows:

$$|Q_{CSi}| \leq \sqrt{S_{CSi}^2 - P_{CSi}^2} \tag{5}$$

where S_{CSi} represents the apparent power of the PHEV charging station at bus i, and its active and reactive power variables at bus i are denoted as P_{CSi} and Q_{CSi}, respectively.

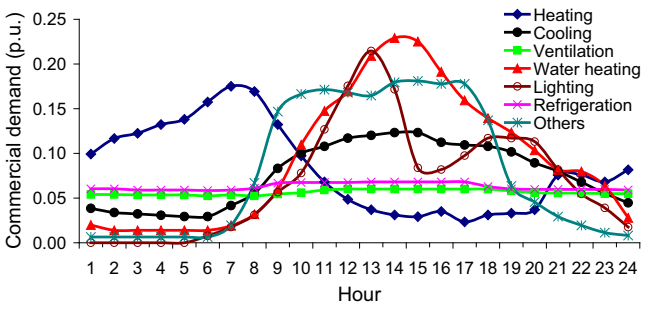

Fig. 1. Normalized daily demand for various commercial load components.

Table 1
Commercial load types and voltage exponents [34–37].

Load types	n_p	n_q	Load types	n_p	n_q
Heating	2.00	0.00	Lighting	1.00	3.00
Cooling	0.50	2.50	Cooking	2.00	0.00
Ventilation	0.08	1.60	Refrigeration	0.50	2.50
Water heating	2.00	0.00	Others	1.51	3.40

Table 2
Charging levels for types of PHEVs [39].

Levels	Input voltage (Vac)	Maximum power (kW)
Normal charging	120	1.44 for all types
Fast charging	240	7.20 for all types
Mixed charging	120	1.44 for sedan
	240	7.20 for SUVs

2.3. Solar PV model

To generate a PV output curve, a probabilistic solar irradiance model employed in previous studies [41,42] is adopted in this work. It is assumed that a day is divided into 24-h periods (*time segments*), each of which has 20 solar irradiance states with a step of 0.05 kW/m^2. The mean and standard deviation values of the hourly solar irradiance are estimated using 3-year historical data [43]. From such data, the probabilities of 20 solar irradiance states for each hour are generated using the Beta Probability Density Function (PDF) model. The PV output powers that correspond to the 20 solar irradiance states for each hour are also calculated using the PV module parameters that can be found in [41].

3. Problem formulation

3.1. Power loss

The total power loss in a distribution network in the absence of charging stations and PV (P_L) can be expressed by (6), widely known as "exact loss formula" [44]:

$$P_L = \sum_{i=1}^{N}\sum_{j=1}^{N}\left[\alpha_{ij}(P_iP_j + Q_iQ_j) + \beta_{ij}(Q_iP_j - P_iQ_j)\right] \quad (6)$$

where $\alpha_{ij} = \frac{r_{ij}}{V_iV_j}\cos(\delta_i - \delta_j)$; $\beta_{ij} = \frac{r_{ij}}{V_iV_j}\sin(\delta_i - \delta_j)$; $V_i\angle\delta_i$ corresponds to the complex voltage at bus i; $r_{ij} + jx_{ij} = Z_{ij}$ denotes the ijth element of impedance matrix $[Z_{bus}]$; P_i and P_j represent the active power injections at buses i and j, respectively; N is the number of buses.

This study considers that a charging station powered by PV units is capable of providing reactive power support to the grid in addition to charging PHEVs at a workplace parking lot. The size of a charging station is calculated as the total power consumed by the aggregated PHEVs. The active and reactive power injected by the PV unit and PHEV charging station at bus i can be described as follows:

$$P_i = P_{PVi} - P_{CSi} - P_{Di} \quad (7)$$

$$Q_i = Q_{PVi} - Q_{CSi} - Q_{Di} \quad (8)$$

where P_{PVi} and Q_{PVi} are the active and reactive power injected by a PV unit at bus i; P_{CSi} and Q_{CSi} are active and reactive power variables of a PHEV charging station at bus i; P_{Di} and Q_{Di} represent the active and reactive load power at bus i, respectively.

Substituting Eqs. (7) and (8) into Eq. (6), we have the total loss in the system with the PV unit and charging station as follows:

$$P_L = \sum_{i=1}^{N}\sum_{j=1}^{N}\left[\alpha_{ij}\left((P_{PVi} - P_{CSi} - P_{Di})P_j + (Q_{PVi} - Q_{CSi} - Q_{Di})Q_j\right) + \beta_{ij}\left((Q_{PVi} - Q_{CSi} - Q_{Di})P_j - (P_{PVi} - P_{CSi} - P_{Di})Q_j\right)\right]. \quad (9)$$

3.2. Energy loss

The total expected power loss over any particular hour period t, $P_L(t)$ (t = 1 h) can be calculated as follows:

$$P_L(t) = \int_0^1 P_L(s)\rho(s)ds \quad (10)$$

where $P_L(s)$ corresponds to the expected P_L at solar irradiance s using Eq. (9); $\rho(s)$ represents the probability of solar irradiance state s in any particular period. Hence, the total daily energy loss in a distribution system, E_L can be derived from Eq. (10) as follows:

$$E_L = \int_0^T P_L(t)dt = \sum_{t=1}^{T} P_L(t) \times \Delta t \quad (11)$$

Here Δt represents the time duration of period t (one hour in this study); T = 24 is the total daily duration time.

4. Analytical approach

4.1. Sizing PHEV charging stations with PV units

In this section, analytical expressions are proposed to size PHEV charging stations in a distribution network with PV units for reducing the power loss. Such a loss is minimized, if the derivative of Eq. (9) with respect to P_{CSi} and Q_{CSi} is equal to zero, described as follows:

$$\frac{\partial P_L}{\partial P_{CSi}} = -2\sum_{j=1}^{N}(\alpha_{ij}P_j - \beta_{ij}Q_j) = 0 \quad (12)$$

$$\frac{\partial P_L}{\partial Q_{CSi}} = -2\sum_{j=1}^{N}(\alpha_{ij}Q_j + \beta_{ij}P_j) = 0 \quad (13)$$

Eqs. (12) and (13) can be rearranged as:

$$\alpha_{ii}P_i + \sum_{j=1, j\neq i}^{N}(\alpha_{ij}P_j - \beta_{ij}Q_j) = 0 \quad (14)$$

$$\alpha_{ii}Q_i + \sum_{j=1, j\neq i}^{N}(\alpha_{ij}Q_j + \beta_{ij}P_j) = 0 \quad (15)$$

Substituting Eqs. (7) and (8) into Eqs. (14) and (15) respectively, we obtain the active and reactive power of the charging station as:

$$P_{CSi} = P_{PVi} - P_{Di} + \frac{1}{\alpha_{ii}}\sum_{j=1, j\neq i}^{N}(\alpha_{ij}P_j - \beta_{ij}Q_j) \quad (16)$$

$$Q_{CSi} = Q_{PVi} - Q_{Di} + \frac{1}{\alpha_{ii}}\sum_{j=1, j\neq i}^{N}(\alpha_{ij}Q_j + \beta_{ij}P_j) \quad (17)$$

The Q_{CSi} at state s within any specific hour period t to minimize the loss can be derived from Eq. (17) as:

$$Q_{CSi(t,s)} = Q_{PVi(t,s)} - Q_{Di(t,s)} + \frac{1}{\alpha_{ii}} \sum_{j=1, j\neq i}^{N} \left(\alpha_{ij} Q_{j(t,s)} + \beta_{ij} P_{j(t,s)}\right) \quad (18)$$

$$Q_{CS}(t) = \int_0^1 Q_{CS}(s)\rho(s)ds \quad (19)$$

4.2. Computational procedure

Given a PHEV location, the size is estimated considering its charging curve by minimizing the energy loss over all periods of a 24-h day as given by Eq. (11). The computational procedure is explained as follows:

Step 1: Analyze load flow for the system with PV units at the average load and find the system loss.
Step 2: Calculate the active power of a PHEV charging station (P_{CSi}) using Eq. (16).
Step 3: Specify the PHEV load for hour period t as below, in which $SF_{CS}(t)$ corresponds to the scaling factor of the PHEV load at period t.

$$P_{CSi}(t) = P_{CSi} \times SF_{CS}(t) \quad (20)$$

Step 4: Analyze load flow for the system with each PHEV load achieved in *Step* 3 for each state. Calculate the reactive power of the charging station for each state using Eq. (18) and the expected reactive power for each period using Eq. (19). Find the energy loss using Eq. (11).

5. Case study

5.1. Test systems

The proposed approach was tested on an 18-bus distribution feeder with a peak load of 1505 kW and 740 kVar, as illustrated in Fig. 2. The voltage bounds are considered to be ±5% of the nominal value. It is assumed that the feeder demand follows a commercial load curve depicted in Fig. 1. The total energy consumed by the feeder over a day is 21.72 MW h. The proposed approach has been simulated in MATLAB. Two PV units that operate at a lagging power factor of 0.95 are connected to the feeder at bus 8 and bus 17 (see Fig. 2). The PDF of each PV module is generated using the model and data presented in Section 2.3.

The assumption is that a charging station is connected to the feeder at bus 17. Such a charging station is used to charge aggregated PHEVs while providing probabilistic reactive power support to the grid within each hour of a 24-h day. Using the model and data reported in Section 2.2, the PDFs of different types of commercial charging load demand: normal, fast and a mix of them is generated and plotted in Fig. 3. Five scenarios are considered in the analysis as follows:

- Base: The feeder without PV units and charging stations
- PV: The feeder with PV units only
- Normal, Fast and Mixed: The feeder including PV units and a charging station with the normal, fast and mixed models, respectively.

5.2. Sizing charging station with mixed charging load model

To evaluate the impact of PHEV adoption considering reactive power support with the time-varying mixed charging load model and PV penetration, the assumption is that the PV penetration level is sized from 0 to 100% with a step of 5%. The penetration level is estimated as the total energy generated by all the PV units divided by the total energy consumed by the feeder over a 24-h day, as previously estimated (21.72 MW h). At each step, the PHEV charging station is sized at bus 17 using the proposed approach given in Section 4 and its corresponding energy loss is calculated. Fig. 4a and b shows the charging station sizes with respect to various PV penetration levels and their corresponding energy losses. The size of the charging station is from minus (−) 0.38 MW to plus (+) 1.04 MW. The positive size indicates that the charging station is being connected to PHEVs and working as a load that is consuming the active power from the grid. In contrast, the negative size shows that the charging station is being connected to PHEVs and working as a generator that is delivering the active power from PHEVs to the grid. It is noted that the charging station is considered in this study to charge PHEVs or consume the active power from the grid; however, the results of the charging station that discharges or delivers the active power are also provided in this subsection for comparison purposes. As shown in Fig. 4b, the loss in the feeder before the PV units and charging station is 0.533 MW h. This amount reduces to a minimum of 0.181 MW h when the PV penetration is 40%. The lowest loss is 0.159 MW h for the case where the feeder accommodates a PV penetration level of 50% and a charging station size of 0.351 MW. Another observation is that the size of the charging station is approximately proportional to the PV generation. However, when the PV penetration is over 45% [see Fig. 4b], the loss further increases and over-voltages occur at a number of buses (e.g., buses 8 and 10) [see Fig. 5a]. Similarly, higher losses and extra voltage drops and/or rises occur when the PV penetration exceeds 55% with the corresponding charging station larger than 0.498 MW [Figs. 4b and 5b]. This is due to a slight mismatch between the PV generation and charging demand. It is noted that the minimum and maximum voltages in Fig. 5a and b are probabilistic values for the whole feeder.

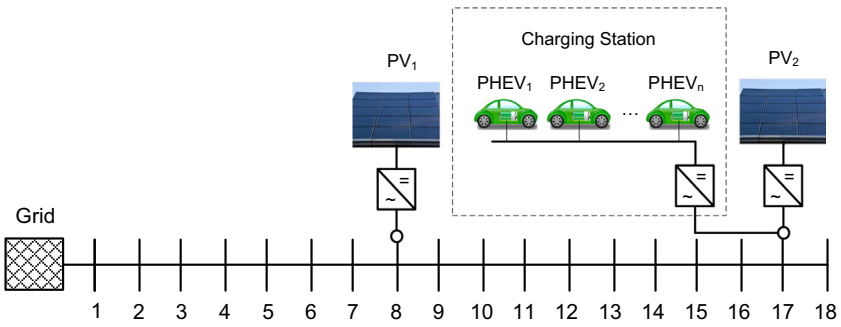

Fig. 2. The 18-bus test feeder with two PV units and a charging station.

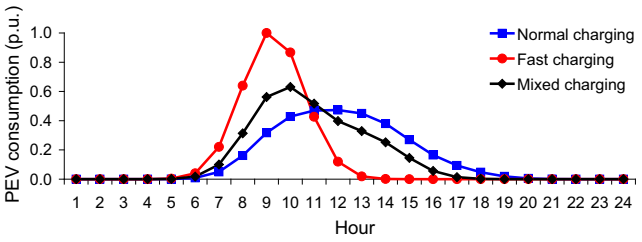

Fig. 3. Normalized daily PHEV charging curves for various load models.

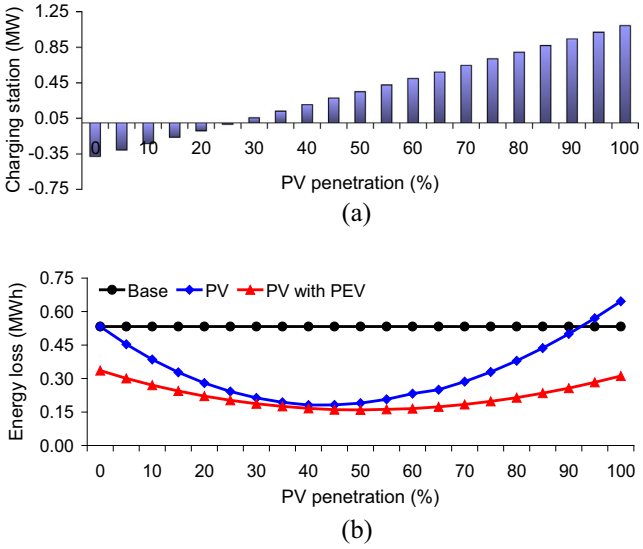

Fig. 4. Sizing PHEV charging stations with respect to various PV penetration levels for the mixed charging load model: (a) the size of a charging station and (b) energy loss.

Fig. 6a–c shows the PDFs of the reactive power response of the PHEV charging station for hour periods 6–19 over the 24-h day. As shown in the figure, the reactive power patterns are different for hours 6–19. Such a difference is owing to the uncertainty/variability of the PV output, load demand and PHEV charging. It is also observed from the figure how the reactive power is controlled over the day using Eq. (18), from minus (–) 0.203 MVAr at hour 11 to plus (+) 0.126 MVAr at hour 16. The negative sign presents that the charging station is injecting its reactive power to the grid, whereas the positive sign presents that the station is consuming the reactive power from the grid. The maximum reactive power of the charging station specified at hour 16 indicates its optimal size, which is 0.203 MVAr.

Fig. 7 presents the hourly energy consumed by the aggregated PHEVs which are plugged in the PHEV charging station at the parking lot over one day (6:00–19:00). This pattern exactly follows the normalized normal charging load as depicted in Fig. 3. The maximum PHEV demand specified at hour 10 is 0.351 MW, the optimal active power of the charging station, which is estimated as the total electricity consumed by all the aggregated PHEVs plugged in the charging station. Fig. 7 also presents the expected reactive power response of the charging station to retain the minimum power loss for each hour of the day. The expected reactive power for each hour is estimated using Eq. (19), where the reactive power states and their corresponding probabilities for each of hours 6–19 are obtained from Fig. 6a–c. It is observed from Fig. 7 that for hours 6–19, the charging station is injecting and absorbing the reactive power in addition to charging PHEVs or consuming the active power from the grid. Without charging at hours 1–5 and 20–24, the station delivers its reactive power. Fig. 8a–c presents the PDFs of the power loss in the feeder in the presence of the station for hours 6–19. As shown in this figure, the power loss patterns are different for such hours. This difference is due to dependence of the power loss on the probability/variability of the load demand, PHEV charging and PV outputs as explained earlier.

Similar to the mixed load model, the next section provides the outcomes for the fast and normal charging load models.

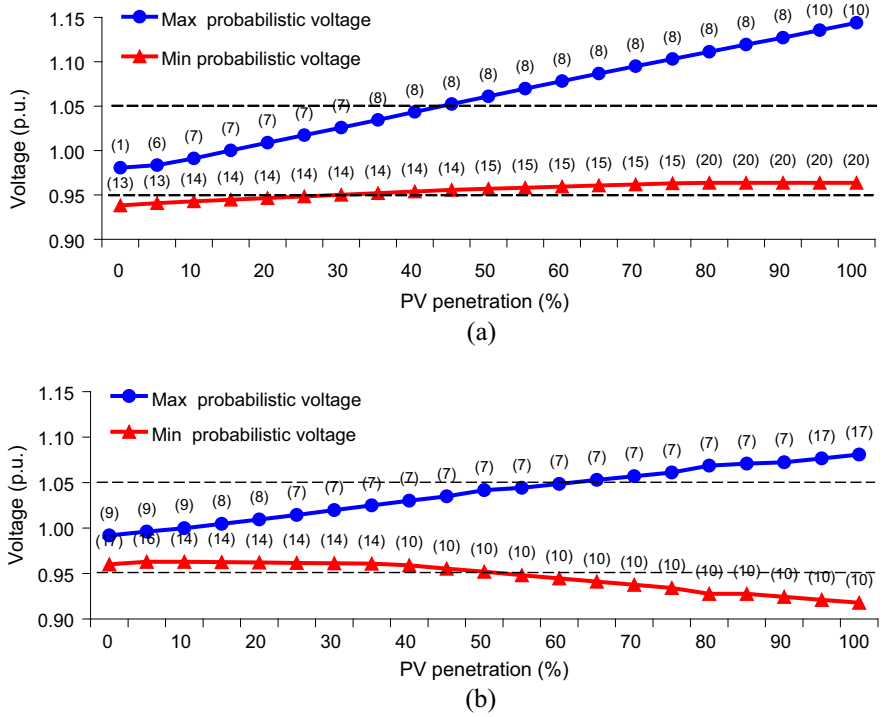

Fig. 5. The voltage distributions for the mixed model in the feeder with: (a) PV and (b) PV with charging station (the value in bracket is hour period).

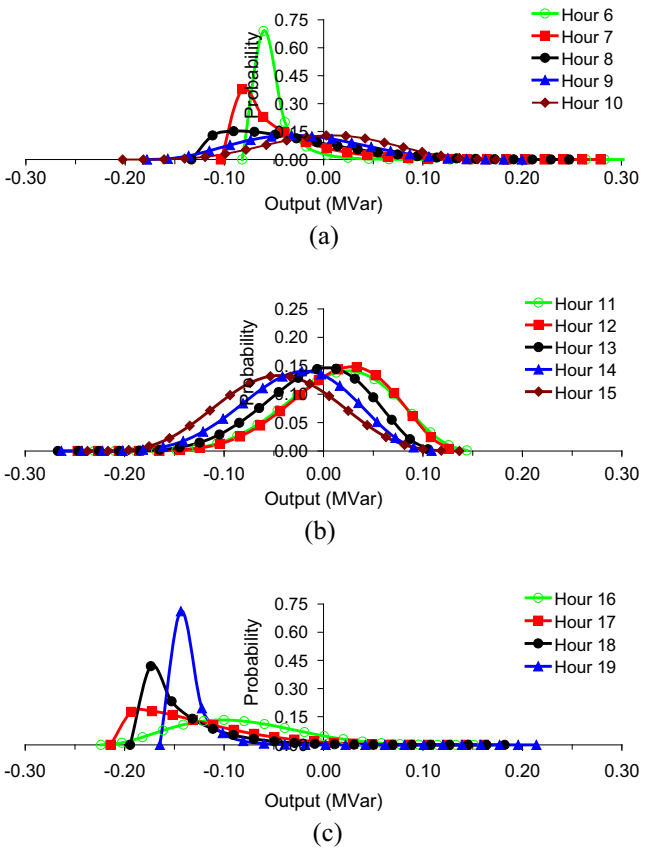

Fig. 6. The probability of the reactive power response of the charging station for the mixed model for various hours: (a) hours 6–10, (b) hours 11–15 and (c) hours 16–19.

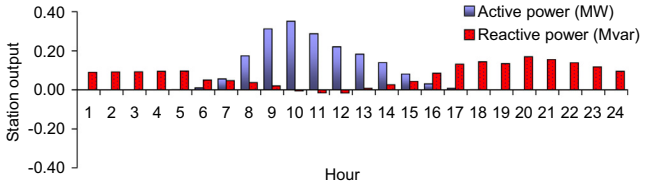

Fig. 7. Hourly expected energy consumption and reactive power response of the charging station at bus 17 for the mixed model.

5.3. Impact of various charging load models

5.3.1. PV penetration

Fig. 9 shows a comparison of the impact of various charging load models on PV penetration and its corresponding charging station for minimizing the energy loss in the feeder. As previously mentioned, without the charging station, the feeder accommodates a PV penetration level of 40%. With the charging station, the PHEV penetration is nearly proportional to the PV generation and dependent on types of charging load models adopted as well. The PHEV penetration is estimated as the total energy consumed by the aggregated PHEVs divided by the total demand as estimated earlier (21.72 MW h). For the fast model, the PV and PHEV penetration levels are lowest at 40% and 3.52% respectively, whereas the respective PV and PHEV levels are highest at 55% and 15.35% for the normal model. This is because the PV generation matches better with the normal charging than the fast charging load pattern. For the mixed model, the PV and PHEV penetration levels are 50% and 9.51%, respectively.

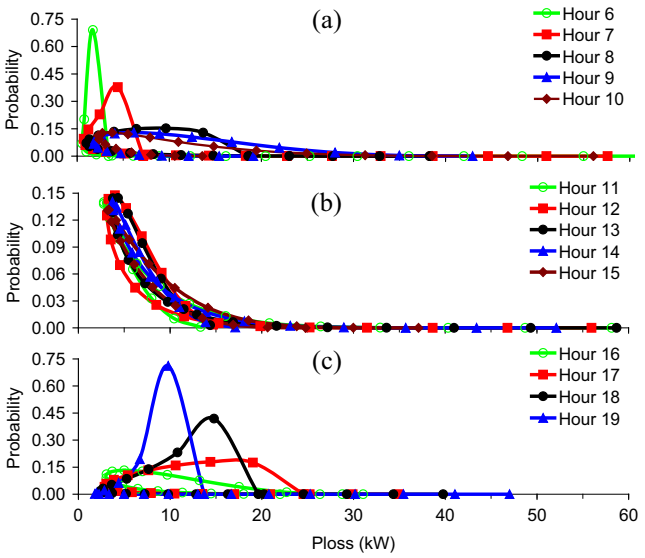

Fig. 8. The probability of the feeder loss with the mixed charging load model for various hours: (a) hours 6–10, (b) hours 11–15 and (c) hours 16–19.

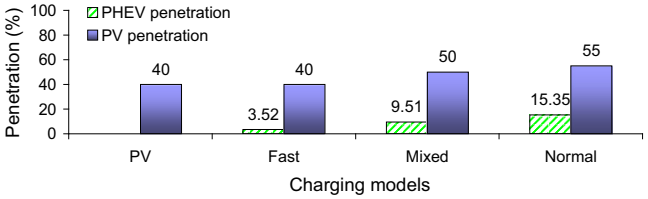

Fig. 9. PV penetration levels with respect to PHEV adoption.

5.3.2. Hourly power losses

Fig. 10 shows the hourly expected power losses with various charging load models. The total expected power loss for each hour period is estimated using Eq. (10), where the power loss states and their corresponding probabilities for each hour are obtained from Fig. 8a–c. For each of hours 1–7 and 10–24, the power loss values for the feeder with the charging station are lower than those without the charging station (i.e., the feeder with two PV units only) due to the PHEVs absorbing the surplus PV generation. This shows that the PHEV charging station positively affects the power losses. In contrast, for a few periods (i.e., hours 8–9), the losses with the charging station is higher than those without the charging station due to the PHEVs consuming a portion of the electricity from the grid.

5.3.3. Peak load

Fig. 11a and b shows the active and reactive load demand of the base case system (i.e., without PV and PHEVs). The demand for each hour of the day is estimated as a sum of all the load components at that hour (see Fig. 1), and the sum is then multiplied by the peak feeder load, plus its corresponding loss. Fig. 11a and b also presents the expected active and reactive power demand of the

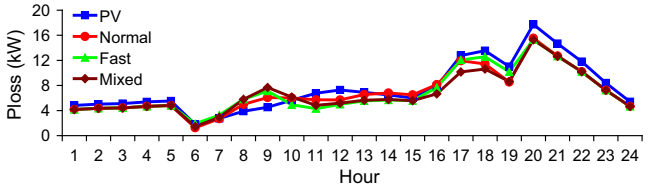

Fig. 10. Hourly expected power losses with different charging load models.

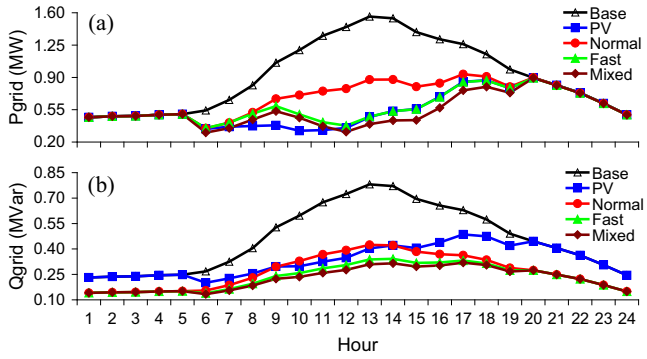

Fig. 11. Hourly load demand of the feeder with PV and PHEV adoption: (a) active power, Pgrid and (b) reactive power, Qgrid.

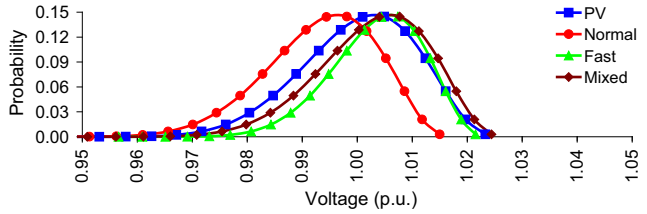

Fig. 12. The PDFs of bus voltages at the PHEV connection point at 13:00.

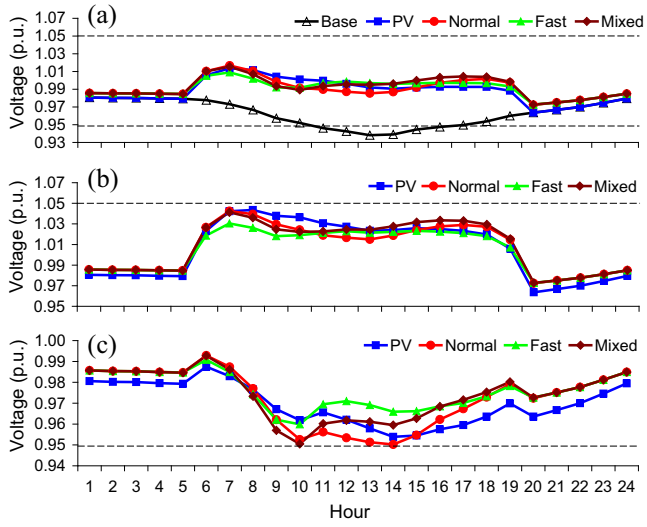

Fig. 13. Hourly voltage distributions at the PHEV connection point (bus 17): (a) mean voltage, (b) maximum voltage, and (c) minimum voltage.

feeder including the probabilistic PV output and energy loss for each hour. A significant reduction in the peak load of the feeder is observed over the day (6:00–19:00). Another observation is that the PHEV charging station added to the feeder with the PV units further reduces the peak load for the charging load models considered. As shown in Fig. 11a, the active power peak load of the feeder reduces from 1.56 MW for the base case to 0.93 MW, 0.89 MW and 0.89 MW for the normal, fast and mixed models, respectively. Similarly, for the reactive power load, these respective figures are 0.42 MVar, 0.34 MVar and 0.32 MVar reduced from 0.78 MVar, as depicted in Fig. 11b.

5.3.4. Voltage profiles

Fig. 12 shows the PDFs of voltages at the connection point of the charging station (bus 17) at 13:00. With the PV and/or charging station, the voltage distribution is within the acceptable limits as assumed earlier. It is noted that the minimum, mean and maximum voltages at hour 13:00 for all the scenarios considered are estimated from Fig. 12. As an example, these values are approximately 0.96 pu, 0.99 pu and 1.02 p.u. respectively for the PV scenario. Similarly, the voltages are obtained for the remaining hours of the day.

Fig. 13a–c shows the probabilistic voltage distribution: minimum, mean and maximum at the connection point of the PHEV charging station over the 24-h day for all the scenarios considered. As shown in Fig. 13a, the mean voltages are under the lower limit of 0.95 p.u. during periods 11–17 for the case without the PV and charging station (i.e., base case). In contrast, with the PV or with the PV and charging station, the mean voltages for all the scenarios improve significantly, as presented in Fig. 13b and c. Another observation is that the minimum and maximum probabilistic voltage distribution are within the permissible limits as shown in such figures.

6. Summary and comparison

Table 3 summarizes the results of PHEV adoption in the feeder with respect to the PV penetration, including the optimal size and capacity of the charging station, where the PV-powered charging station is capable of providing reactive power support in compliance with the latest version of the standard IEEE 1547 recently published [40] and the newest German and Italian codes as well [45,46]. Table 3 also shows a comparison of the daily feeder energy losses before and after the PV and charging station connected with different time-varying charging load models. The daily energy loss is estimated using Eq. (11), where the energy loss for each hour can be obtained from Fig. 10. As shown in the table, the energy loss in the initial feeder (i.e., base case) is 0.533 MW h. This amount reduces to 0.181 MW h after the two PV units are connected. Lower losses, at roughly 0.160 MW h are achieved for the scenarios where both PV units and charging station are considered. In addition, the

Table 3
PHEV adoption with consideration of reactive power support for various charging load models.

Scenarios	Base	PV	PV and charging station		
			Normal	Fast	Mixed
PV penetration (%)		40	55	40	50
PHEV penetration (%)			15.35	3.52	9.51
Charging station size (MW)			0.425	0.204	0.351
Charging station size (MVar)			0.199	0.195	0.203
Capacity (MW h)			3.334	0.758	2.065
Energy loss (MW h)	0.533	0.181	0.165	0.164	0.159
Loss reduction (%)		66.04	69.04	69.23	70.17
Peak load (MW)	1.56	0.90	0.93	0.89	0.89
Peak load (MVar)	0.78	0.49	0.42	0.34	0.32

Table 4
PHEV adoption without consideration of reactive power support for various charging load models.

Scenarios	Base	PV	PV and charging station		
			Normal	Fast	Mixed
PV penetration (%)		40	50	35	45
PHEV penetration (%)			12.69	2.24	7.52
Charging station size (MW)			0.354	0.133	0.280
Charging station size (MVar)			0	0	0
Capacity (MW h)			2.756	0.487	1.633
Energy loss (MW h)	0.533	0.237	0.237	0.239	0.235
Loss reduction (%)		55.51	55.60	55.12	55.83
Peak load (MW)	1.56	0.90	0.93	0.90	0.90
Peak load (MVar)	0.78	0.75	0.75	0.75	0.75

peak active and reactive power loads in the system for all the scenarios are summarized in Table 3.

To validate the novelty and effectiveness of the results obtained from the proposed approach reported in Table 3, Table 4 provides a summary of the results of PV-powered PHEV charging stations without consideration of reactive power support under the recommendation of the previous version of the standard IEEE 1547 [47]. It is observed from Table 4 that without reactive power provision, the system accommodates lower penetration levels of PV and PHEVs for all the charging load models adopted than those provided in Table 3, where the reactive power support is considered. These lower penetration levels occur due to an inadequacy of local reactive power support or voltage support in the system. In this circumstance, the loads are consuming a large amount of reactive power provided from the source (bus 1), thereby resulting in an excessive increase in network energy losses for all the scenarios with exclusion of reactive power support, as tabulated in Table 4. The simulation carried out in this study has also observed that an attempt to increase the amount of PHEV charging loads in the above scenarios leads to voltage violations, namely voltage drops at a large number of buses in the system below the lower limit along with higher network energy losses. This finding implies that the standards and regulatory frameworks regarding PV and PHEV planning and operations need to be revised in compliance with the recently published amendment to the standard IEEE 1547 [40].

7. Conclusion

This paper has proposed a new analytical approach to determine the size of PHEV charging stations powered by various levels of commercial grid-connected PV penetration that considers probabilistic reactive power support for minimizing energy losses. The advantage of the proposed approach is that it can provide a quick estimation of the optimal size of PV-powered charging stations and their probabilistic reactive power support. These stations are capable of providing reactive power support to the grid in addition to charging PHEVs. The proposed approach has been further extended to study the impact of various time-varying voltage-dependent commercial charging load levels on PV penetration. The results show that without charging stations, an 18-bus distribution feeder can accommodate a PV penetration level of 40%. With charging stations, a higher level of 55% and 15.35% for respective PV and PHEVs can be achieved when the normal charging load model is adopted. However, due to a mismatch between the charging demand and PV generation, the fast charging load model cannot enable higher PV penetration while adopting a rather low amount of PHEVs, at 3.52%. Moreover, a practical or mixed load charging model that is defined as a mix of the fast and normal models has been examined. For this model, the penetration levels of respective PV and PHEVs are 50% and 9.50%, and the largest reductions in the energy loss and peak active load are estimated at 70.17% and 42.95%, respectively.

The simulation results also confirm that optimal sizing and operation of PV-powered charging stations with reactive power support, which is fully compliant with a recently published amendment to the standard IEEE 1547, can lead to a significantly lower energy loss, higher levels of PV and PHEV penetration and a higher peak load reduction than the scenario without consideration of reactive power support. Accordingly, the proposed approach could be a useful study tool to support daytime workplace charging that absorbs energy produced by solar PV panels and to facilitate higher penetration levels of PV and PHEVs in distribution networks.

References

[1] Global market outlook for solar power; 2015–2019. http://resources.solarbusinesshub.com/solar-industry-reports/item/global-market-outlook-for-solar-power-2015-2019.
[2] IEA. Global EV outlook: understanding the electric vehicle landscape to 2020. https://www.iea.org/publications/globalevoutlook_2013.pdf.
[3] Nienhueser IA, Qiu Y. Economic and environmental impacts of providing renewable energy for electric vehicle charging – a choice experiment study. Appl Energy 2016;180:256–68.
[4] Hen-Geul Y, Gayme DF, Low SH. Adaptive VAR control for distribution circuits with photovoltaic generators. IEEE Trans Power Syst 2012;27(3):1656–63.
[5] Richardson P, Flynn D, Keane A. Optimal charging of electric vehicles in low-voltage distribution systems. IEEE Trans Power Syst 2012;27(1):268–79.
[6] Traube J, Lu F, Maksimovic D, Mossoba J, Kromer M, Faill P, et al. Mitigation of solar irradiance intermittency in photovoltaic power systems with integrated electric-vehicle charging functionality. IEEE Trans Power Electr 2013;28(6):3058–67.
[7] Karan E, Mohammadpour A, Asadi S. Integrating building and transportation energy use to design a comprehensive greenhouse gas mitigation strategy. Appl Energy 2016;165:234–43.
[8] Birnie Iii DP. Solar-to-vehicle (S2V) systems for powering commuters of the future. J Power Sources 2009;186(2):539–42.
[9] Nunes P, Farias T, Brito MC. Day charging electric vehicles with excess solar electricity for a sustainable energy system. Energy 2015;80:263–74.
[10] Nunes P, Farias T, Brito MC. Enabling solar electricity with electric vehicles smart charging. Energy 2015;87:10–20.
[11] Tulpule PJ, Marano V, Yurkovich S, Rizzoni G. Economic and environmental impacts of a PV powered workplace parking garage charging station. Appl Energy 2013;108:323–32.
[12] Denholm P, Kuss M, Margolis RM. Co-benefits of large scale plug-in hybrid electric vehicle and solar PV deployment. J Power Sources 2013;236:350–6.
[13] Ma T, Mohammed O. Optimal charging of plug-in electric vehicles for a car park infrastructure. IEEE Trans Ind Appl 2014;50(4):2323–30.
[14] Mohamed A, Salehi V, Ma T, Mohammed O. Real-time energy management algorithm for plug-in hybrid electric vehicle charging parks involving sustainable energy. IEEE Trans Sustain Energy 2014;5(2):577–86.
[15] Wi YM, Lee JU, Joo SK. Electric vehicle charging method for smart homes/buildings with a photovoltaic system. IEEE Trans Consumer Electr 2013;59(2):323–8.
[16] Stadler M, Kloess M, Groissböck M, Cardoso G, Sharma R, Bozchalui MC, et al. Electric storage in California's commercial buildings. Appl Energy 2013;104:711–22.
[17] Yamagata Y, Seya H. Simulating a future smart city: an integrated land use-energy model. Appl Energy 2013;112:1466–74.
[18] Liu N, Chen Q, Liu J, Lu X, Li P, Lei J, et al. A Heuristic operation strategy for commercial building microgrids containing EVs and PV system. IEEE Trans Ind Electr 2015;62(4):2560–70.

[19] Chandra Mouli GR, Bauer P, Zeman M. System design for a solar powered electric vehicle charging station for workplaces. Appl Energy 2016;168:434–43.
[20] Chaouachi A, Bompard E, Fulli G, Masera M, De Gennaro M, Paffumi E. Assessment framework for EV and PV synergies in emerging distribution systems. Renew Sustain Energy Rev 2016;55:719–28.
[21] Liu N, Zou F, Wang L, Wang C, Chen Z, Chen Q. Online energy management of PV-assisted charging station under time-of-use pricing. Electr Power Syst Res 2016;137:76–85.
[22] Van Der Kam M, Van Sark W. Smart charging of electric vehicles with photovoltaic power and vehicle-to-grid technology in a microgrid; a case study. Appl Energy 2015;152:20–30.
[23] Tushar W, Yuen C, Huang S, Smith DB, Poor HV. Cost minimization of charging stations with photovoltaics: an approach with EV classification. IEEE Trans Intell Transp Syst 2016;17:156–69.
[24] Guo Y, Xiong J, Xu S, Su W. Two-stage economic operation of microgrid-like electric vehicle parking deck. IEEE Trans Smart Grid 2016;7:1703–12.
[25] Capasso C, Veneri O. Experimental study of a DC charging station for full electric and plug in hybrid vehicles. Appl Energy 2015;152:131–42.
[26] Goli P, Shireen W. PV powered smart charging station for PHEVs. Renew Energy 2014;66:280–7.
[27] Tovilović DM, Rajaković NLJ. The simultaneous impact of photovoltaic systems and plug-in electric vehicles on the daily load and voltage profiles and the harmonic voltage distortions in urban distribution systems. Renew Energy 2015;76:454–64.
[28] Turitsyn K, Sulc P, Backhaus S, Chertkov M. Options for control of reactive power by distributed photovoltaic generators. Proc IEEE 2011;99(6):1063–73.
[29] Thomson M, Infield DG. Network power-flow analysis for a high penetration of distributed generation. IEEE Trans Power Syst 2007;22(3):1157–62.
[30] Samadi A, Ghandhari M, Söder L. Reactive power dynamic assessment of a PV system in a distribution grid. Energy Procedia 2012;20:98–107.
[31] Kesler M, Kisacikoglu MC, Tolbert LM. Vehicle-to-grid reactive power operation using plug-in electric vehicle bidirectional off board charger. IEEE Trans Ind Electr 2014;61(12):6778–84.
[32] Acharya N, Mahat P, Mithulananthan N. An analytical approach for DG allocation in primary distribution network. Int J Elect Power Energy Syst 2006;28(10):669–78.
[33] Alternative sectoral load shapes for NEMS; August 2001. Available: http://www.onlocationinc.com/LoadShapesAlternative2001.pdf.
[34] Asper SG, Nwankpa CO, Bradish RW, Chiang HD, Concordia C, Staron JV, et al. Bibliography on load models for power flow and dynamic performance simulation. IEEE Trans Power Syst 1995;10(1):523–38.
[35] Cutsem TV, Vournas C. Voltage stability of electric power systems. Power Electronics and Power System Series: Kluwer; 1998.
[36] Taylor CW. Power system voltage stability. Electric Power Research Institute: McGraw-Hill; 1994.
[37] Eminoglu U, Hocaoglu MH. A new power flow method for radial distribution systems including voltage dependent load models. Electr Power Syst Res 2005;76(1–3):106–14.
[38] Darabi Z, Ferdowsi M. Aggregated impact of plug-in hybrid electric vehicles on electricity demand profile. IEEE Trans Sustain Energy 2011;2(2):501–8.
[39] J1772 SS. SAE electric vehicle conductive charge coupler; 2001.
[40] IEEE standard for interconnecting distributed resources with electric power systems – Amendment 1. IEEE Std 1547a–2014 (Amendment to IEEE Std 1547–2003); 2014. p. 1–16.
[41] Hung DQ, Mithulananthan N, Lee KY. Determining PV penetration for distribution systems with time-varying load models. IEEE Trans Power Syst 2014;29(6):3048–57.
[42] Hung DQ, Mithulananthan N, Bansal RC. Integration of PV and BES units in commercial distribution systems considering energy loss and voltage stability. Appl Energy 2014;113:1162–70.
[43] SolarAnywhere. https://solaranywhere.com [accessed 01/03/2016].
[44] Elgerd IO. Electric energy system theory: an introduction. New York: McGraw-Hill Inc.; 1971.
[45] Generators connected to the LV distribution network—technical requirements for the connection to and parallel operation with low-voltage distribution networks. VDE Standard VDE-AR-N 4105; 2011.
[46] Reference technical rules for connecting active and passive users to networks low-voltage electricity networks of energy providers. CEI Standard CEI 0-21; 2011.
[47] IEEE 1547 standard for interconnecting distributed resources with electric power systems; October 2003.